Chapter

Three-Dimensionally Ordered Macroporous-Mesoporous Bioactive Glass Ceramics for Drug Delivery Capacity and Evaluation of Drug Release

Reedwan Bin Zafar Auniq, Namon Hirun and Upsorn Boonyang

Abstract

Bioactive glass ceramics (BGCs) have been used in orthopedic and dentistry due to having better osteoconductive and osteostimulative properties. This study aimed to evaluate and compare the drug release properties of two different BGCs; 45S5 and S53P4. The BGCs were composed with four phases of SiO_2 – CaO – Na_2O – P_2O_5 system, synthesized by sol–gel method using dual templates; a block-copolymer as mesoporous templates and polymer colloidal crystals as macroporous templates, called three-dimensionally ordered macroporous-mesoporous bioactive glass ceramics (3DOM-MBGCs). *In vitro* bioactivity test performed by soaking the 3DOM-MBGCs in simulated body fluid (SBF) at 37°C. The results indicated that, the 45S5 have the ability to grow hydroxyapatite-like layer on the surfaces faster than S53P4. Gentamicin drug was used to examine *in vitro* drug release properties in phosphate buffer solution (PBS). The amount of drug release was quantified through UV/Vis spectroscopy by using *o*-phthaldialdehyde reagent. S53P4 showed high drug loading content. The outcome of drug release in PBS showed that both S53P4 and 45S5 exhibited a slowly continuous gentamicin release. The resultant drug release profiles were fitted to the Peppas-Korsmeyer model to establish the predominant drug release mechanisms, which revealed that the kinetics of drug release from the glasses mostly dominated by Fickian diffusion mechanism.

Keywords: macroporous, mesoporous, ceramics, bioactive glasses, drug release, sol–gel process

1. Introduction

Bone is the second most widely transplanted tissue after blood. More than 2.2 million bone graft operations are performed annually worldwide in order to repair bone defects in orthopedics and dentistry [1]. Bioactive glass ceramics (BGCs) are one of the most promising synthetic bone replacements come regeneration material which has the ability to chemically bond with living bone tissue and stimulate bone

growth without promoting inflammation or toxicity, developed by Larry Hench at the University of Florida in 1969 [1–4]. In early the heated glass powder, the micro-composite between apatite and β-wollastonite ($CaO{\cdot}SiO_2$) within a homogenous glassy phase showed not only a bioactivity but also high mechanical strength [4]. This BGCs was called A/W derived from the names of crystalline phase. The bioactivity of glass ceramics is believed to be due to the dissolution of calcium from wollastonite and/or the glassy phase. In case of treating bone defect, the bone regeneration rate depends on the material's composition [5]. Hydroxyapatite (HA) is the inorganic part of human bone [6]. The bonding with bone process is associated with the formation of HA layer on the implant's surface [7]. BGCs can either be synthesized by the melt quenching or sol–gel method. Early BGCs were prepared by the melt quenching method. Sol–gel processing was started practicing in early 1990s for bioactive glass synthesis. Sol–gel derived bioactive glasses are made of a colloidal silica solution synthesized by the hydrolysis of alkoxide precursor to form a sol. Tetraethyl orthosilicate (TEOS) is commonly used as silica precursor, Triethyl phosphate (TEP) is used to add phosphate, salt calcium nitrate used to introduce calcium and Na_2O included to decrease the melting temperature [8, 9]. Sol–gel derived bioactive glasses can provide higher surface Si-OH groups, which promote active places for more functionalization. The greater specific surface area that enhance the rate of hydroxyapatite formation is considerably higher degree of bioactivity compare to the melt quenching process [10–12]. Mesoporous bioactive glass ceramics (MBGCs) are considered the third-generation bioactive glasses were developed in 2004 by the combination of sol–gel method. MBGCs can possess more optimal surface area, ordered mesoporous structure, variable pore size and volume, improved in *in vitro* apatite mineralization in simulated body fluid (SBF) comparing with non-mesoporous bioactive glasses (NBG) [13]. However, BGCs having higher specific surface area and pore volume accelerates the hydroxyapatite formation and increase prolong the bioactive behavior [9]. MBGCs also get focused because of having more potential applications, such as catalysis, adsorption/separation, nanomaterial synthesis and also in biomaterial science as bone scaffolds for drug delivery and bone regeneration [9].

Mesoporous bioactive glass ceramic (MBGC) has brought a significant revolution in material science in terms of drug delivery. MBGC has some important properties which make itself more potential for drug delivery, such as well-ordered pores, large pore volumes and high specific surface area. As a result, MBGCs can easily entrap the drug molecules with its highly ordered mesoporous channel with a pore range of 2 to 50 nm [12, 14–17]. These characteristics greatly enhance MBGC for bone forming bioactivity, higher drug loading efficiency and lower drug release kinetics comparing with conventional BGCs [18–21]. Moreover, the mesosized pore are too small to promote cell growth. To overcome this limitation, the macroporous networks was studied and it suitable for tissue scaffolds that mimic the structure of porous bone structure [1].

Sol–gel technology is a wonderful progression in science with various applications since 1800s [12]. It is the process of making ceramic and glass materials using relatively low temperature hydrolysis and condensation reaction followed aging, drying and thermal stabilization [1]. Use of different surfactants (eg: P123, F127) during MBGCs preparation amplify the pore volume and surface area, which enhance the drug loading efficiency [16]. 45S5 and S53P4 bioactive glasses with a system of SiO_2-Na_2O-CaO-P_2O_5 considered more attention for bone tissue regeneration and regeneration properties due to their excellent bioactivity, biocompatibility, osteogenic and angiogenic effects [4, 18, 22–24]. Perioglas® was the first commercial product of 45S5 glasses, later reestablished by NovaBone® and BoneAlive® commercialized with composition of S53P4 [4].

Conventional treatment of bone infections like osteomyelitis involves surgery to remove necrotic bone tissue and repeated irrigations combined with the use of

systemic antibiotics administration, wound drainage and implant removal. Systemic therapy of antibiotics has various adverse effects and risk of developing bacterial resistance to drugs. Local drug delivery system solves the problems by providing more advantages including high drug delivery efficiency, continuous action, reduced toxicity and convenience to the patients. Administration of single dose of localized drug with desired therapeutic range can reduce the need for follow-up care, reduce the risk of side effects, toxicity and increase patient compliance [19, 20, 25].

In our study, the hierarchically macroporous structured and mesosized pores of 45S5 and S53P4 BGCs were synthesized by sol–gel method and evaluated their *in vitro* bioactivity. The bioactivity effects of both bioactive glasses were investigated in SBF solution. The *in vitro* drug release properties in PBS were evaluated. Gentamicin sulfate (GS) was chosen as a model drug to encapsulation in the MBGCs to obtain a drug delivery system. GS is a broad-spectrum bactericidal antibiotic belonging aminoglycoside class; antibacterial activity is due to its ability to irreversibly bind ribosomes and half bacterial protein synthesis. GS vastly used in orthopedic treatments [26–28].

2. Experimental

2.1 Materials

Calcium nitrate tetrahydrate (CNT; $Ca(NO_3)_2.4H_2O$), tetraethyl orthosilicate (TEOS; $Si(OC_4H_9)_4$, 98%), triethyl phosphate (TEP; $P(OEt)_3$, 99%) were purchased from Acros Organic, sodium nitrate ($NaNO_3$), nitric acid (HNO_3) were purchased from Merck, Germany, the surfactant Pluronic P123 (EO_{20}-PO_{70}-EO_{20}, average Mn ~ 5800) were produced from Sigma-Aldrich, Germany. Gentamicin was obtained from Fuan Pharmaceutical group Yantai Co., LTD. Polymethylmethacrylate (PMMA) colloidal crystals with 300 nm size were prepared by our previous worked [29].

2.2 Preparation of bioactive glass ceramics

Two different 3DOM-MBGCs; 45S5 and S53P4 were synthesized *via* sol–gel method follow by published work [30]. The synthesis process went through hydrolysis and polycondensation of TEOS, TEP, CNT and $NaNO_3$ (**Figure 1**) with the appropriate mol ratio mentioned in **Table 1**. HNO_3 was used to catalyze the hydrolysis process and non-ionic block copolymer P123 was chosen as structure-directing agent. The solution was vigorously stirred (700 rpm) at room temperature to obtain a clear sol (hydrolysis reaction) and further stirred to reach the gel point (condensation reaction). To obtain 3DOM structure, a monolithic piece of the PMMA colloidal crystal templates were completely immersed in the sol and excess solution was removed. The products were aged in sealed vials at 45°C for 24 h to allow the polycondensation reaction followed by a drying process at 45°C for 24 h to eliminate excess solvents and by products. Finally, the samples were stabilized at 600°C in air for 4 h with a fixed heating rate of 2°C/min. The morphology of the bioactive glasses was analyzed in detail by scanning electron microscopy (SEM). Their element compositions were characterized by energy dispersive spectroscopy (EDS) attached to the SEM with Silicon crystal detectors. Fourier Transform Infrared Spectroscopy (FTIR) was carried out in the transmission mode with mid-infrared range 400–4000 cm^{-1} at a resolution of 4 cm^{-1} by using the KBr pellet method. The N_2 adsorption–desorption measurements carried out by Brunauer–Emmett–Teller (BET) for surface area analysis and Barrett–Joyner–Halenda (BJH) for pore size and volume analysis.

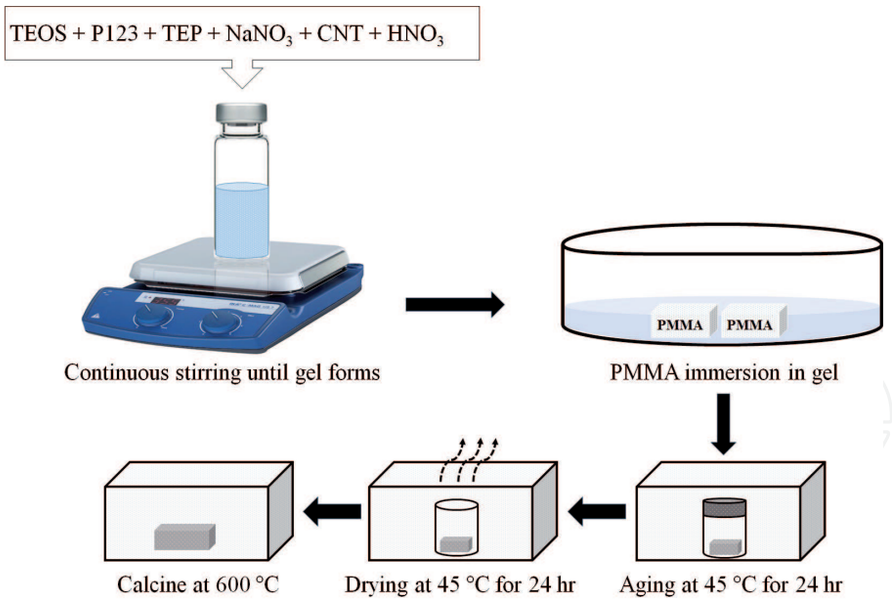

Figure 1.
Synthesis of 3DOM-MBGCs via sol–gel method.

Reagents	Compositions	
	45S5	S53P4
TEOS ($SiC_8H_{20}O_4$)	45% SiO_2	53% SiO_2
TEP ($C_6H_{15}O_4P$)	6% P_2O_5	4% P_2O_5
$Ca(NO_3)_2.4H_2O$	24.5% CaO	20% CaO
$NaNO_3$	24.5% Na_2O	23% Na_2O

Table 1.
Chemicals used in synthesis of 45S5 and S53P4 3DOM-MBGCs.

2.3 Assessment of *in vitro* bioactivity test

The bioactivity of the obtained samples was examined using *in vitro* test by immerging the samples in SBF solution at body temperature, 37°C at pH 7.40 following Kokubo method [31]. The *in vitro* bioactivity was performed by soaking grainy 3DOM-MBGCs in the SBF solution at a temperature of 37.0°C for 1, 2, 3 and 7 days with daily refreshing of the SBF solution. The ratio of the glass powders weight to SBF volume was 1.5 mg/mL. After soaking, samples were removed from the SBF solution and washed with deionized water several times and air-dried at room temperature. The changes of the bioactive glass surfaces were examined by SEM and FTIR techniques.

2.4 *In vitro* study of drug release

2.4.1 Determination of drug concentration

Gentamicin concentration was analyzed by measuring the UV/Vis absorbance of gentamicin-*o*-phthaldialdehyde complex at 333 nm [14]. The *o*-phthaldialdehyde reagent was prepared according to Huang et al., 2017 [17]. 1 mL of gentamicin solution, 1 mL of isopropanol and 1 mL of *o*-phthaldialdehyde reagent were reacted for 45 min at room temperature to prepare the sample to examine in UV/visible

spectroscopy [32]. Before determination, a calibration curve (R^2 = 0.99) was made for each set of measurements and determined by taking absorbance vs. drug concentration between 1 to 150 ppm as parameters.

2.4.2 Encapsulation of gentamicin in the bioactive glass ceramics

Encapsulation of gentamicin into the MBGCs (45S5 and S53P4) were carried out in PBS pH 7.4 at room temperature for 24 h. 200 mg of each MBGCs was immersed in 10 mL of PBS containing gentamicin with a concentration of 10 mg/mL and stirred for 24 h. After that, the drug loaded MBGCs were filtered and then the drug loading efficiency and drug loading content were determined. Drug loading efficiency was measured by depletion method, by determining the difference in gentamicin concentration in the loading medium before and after loading [14]. The drug-loading experiments were carried out in triplicate, and the statistical computations were performed with the IBM SPSS Statistics version 25. Drug loading efficiency and drug loading content are two important parameters for drug delivery study with MBGCs. Drug loading content represents the mass ratio of drugs in drug loaded MBGCs and drug loading efficiency reflects the utilization of drugs in feed during drug loading [33]. The drug loading efficiency and drug loading content are expressed according to the following Equations [33].

$$\text{Drug loading efficiency}(wt.\%) = \frac{\text{Mass of the drug in MBGCs}}{\text{Mass of the drug in feed}} x100 \quad (1)$$

$$\text{Drug loading content}(wt.\%) = \frac{\text{Mass of the drug in MBGCs}}{\text{Initial mass of MBGCs}} x100 \quad (2)$$

2.4.3 In vitro drug release

50 mg of drug loaded MBGCs were placed into 10 mL of PBS and subsequently agitated in a horizontal shaking incubator at 37°C. 2 mL of release medium was withdrawn at predetermined time intervals and replaced with fresh release medium (2 mL) at each measurement. The triplicate samples of each drug loaded MBGCs (45S5 and S53P4) were used to determine the drug release profile.

2.4.4 Kinetic analysis drug release profile

To study the drug release kinetic from 45S5 and S53P4 MBGCs, the *in vitro* drug release data of gentamicin was fitted in Peppas-Korsmeyer kinetic model mentioned below;

$$\frac{M_t}{M_\infty} = Kt^n \quad (3)$$

Where K is the Peppas-Korsmeyer constant, $\frac{M_t}{M_\infty}$ is the fractional solute release at time t, and n is the exponent indicative of the release mechanism. An exponential value in the range of 0.45 or less and 0.89 or above indicate respectively Fickian

diffusion and case II transport (typical zero-order release). Values between 0.45 and 0.89 indicate non-Fickian or anomalous release by both diffusion and erosion release [34].

3. Results and discussion

3.1 Morphology and microstructure of bioactive glass ceramics

Figure 2 shows the SEM image and EDS spectra of (a) 45S5 and (b) S53P4 3DOM-MBGCs. Bioactive glass with hierarchical porosity was formed through the PMMA and Pluronic P123 dual templating system. The SEM image of 53S4P (**Figure 2(b)**) shows more well ordered macroporous structure with spherical pores are around 300 nm. While, 45S5 shows distorted 3DOM structure (**Figure 2(a)**). The EDS spectrum of 45S5 and S53P4 in **Figure 2** shows the peaks corresponding to Si, Ca, Na and O that represent the preservation of the elements in the precursors without impurity elements. The FTIR spectra of 45S5 and S53P4 3DOM-MBGCs in **Figure 3** exhibits the characteristic peaks of Si-O-Si bending, symmetric and asymmetric stretching vibration at 467, 802 and 1086 cm^{-1}, respectively. In the peak at 564 and 950 cm^{-1} corresponding to the P-O bending and stretching vibration, respectively. In addition, the peak at 1635 and 3450 cm^{-1} correlates to O-H bonds indicates the water trapped inside the sample. The narrow band near 1384 cm^{-1} indicates the characteristic of the carbonate group (CO_3^{2-}) [35]. **Figure 4** indicates that all the BET curves of the 45S5 and S53P4 MBGCs presented a type IV isotherms

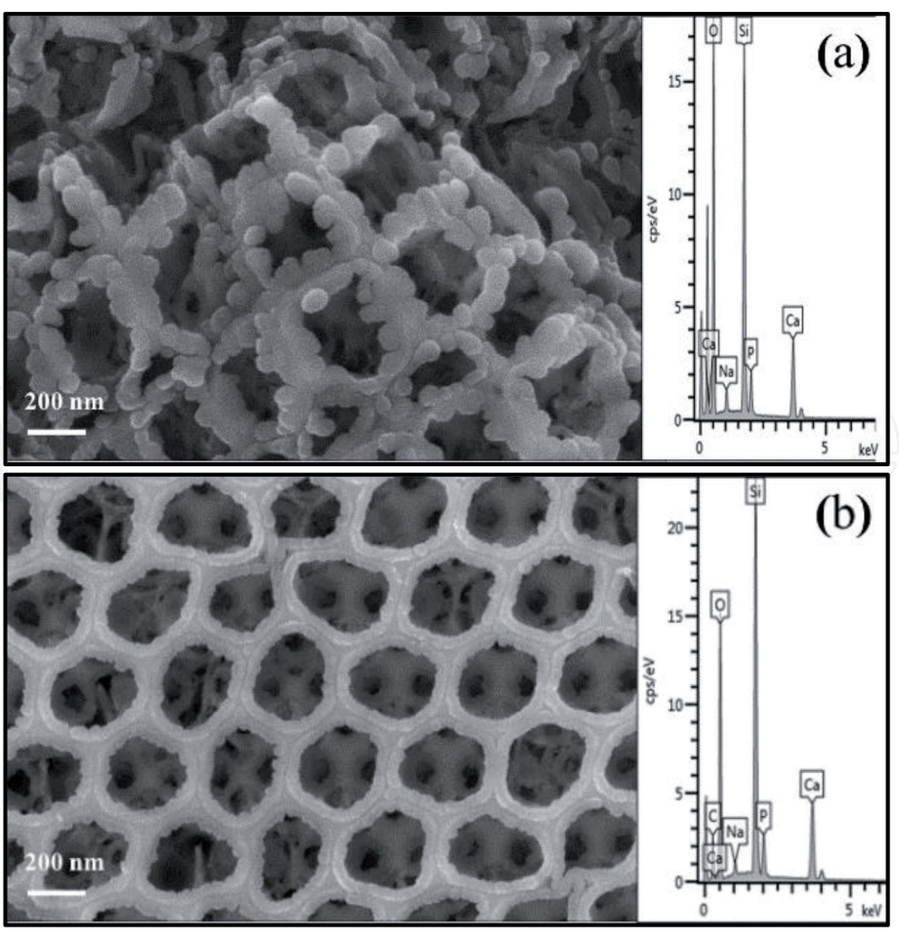

Figure 2.
SEM and EDS spectra of (a) 45S5 and (b) S53P4 3DOM-MBGCs.

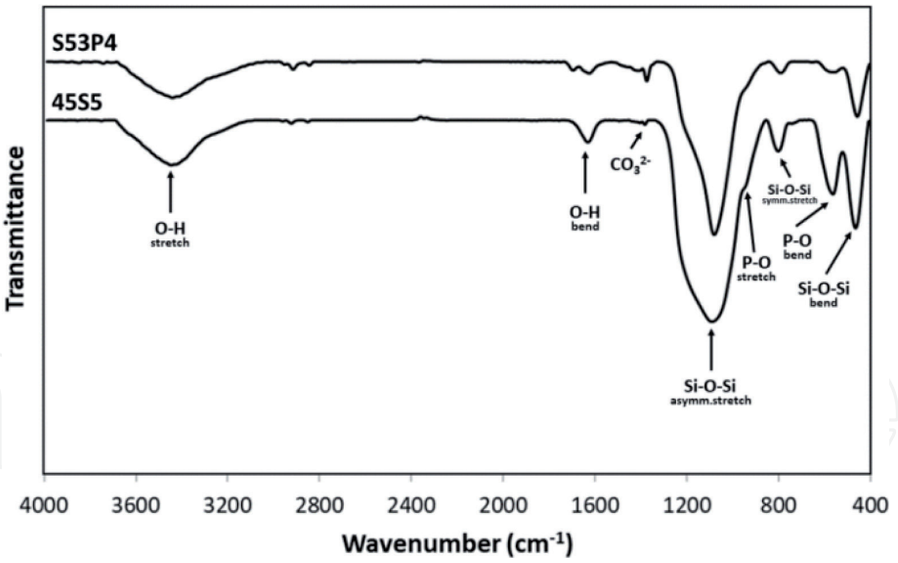

Figure 3.
FTIR spectra of (a) 45S5 and (b) S53P4 3DOM-MBGCs. Copyright [30].

pattern with type H4 hysteresis loops, characterizing mesoporous materials with narrow slit-like pores, with internal voids of irregular shape and broad size distribution [36]. This is confirmed by the average data of specific surface area, pore volume and pore diameter of 45S5 and S53P4 3DOM-MBGCs listed in **Table 2**. The bioactive glasses show specific surface area in range of 96.54 to 116.76 m^2/g. The 45S5 glasses shows a relatively wide pore size distribution calculated from the adsorption branch using the BJH model, and the average pore size is around 15.158 nm, while the S53P4 glasses gained average pore size around 11.230 nm.

3.2 Assessment of *in vitro* bioactivity test

The *in vitro* bioactivity of 3DOM-MBGCs was tested at body temperature of 37°C by using the SBF solution whose composition and ionic concentration similar to human blood plasma. **Figure 5** shows the SEM images of 45S5 bioactive glasses having different soaking time in SBF solutions. Compared with the morphology of the prepared bioactive glasses in **Figure 5a**, the nucleation of hydroxyapatite occurred on the glass surfaces after soaking in the SBF solution for 2 days (**Figure 5c**). The surface of 45S5 glasses were covered by precipitation of apatite-like layer more than 3 days soaking in SBF solution (**Figure 5d-f**). **Figure 6**, the formation of hydroxyapatite-like on the surface of S53P4 glasses started after 3 days of immersion in SBF solution. Within 7 days, most of the glass surfaces were covered by the apatite-like layer (**Figure 6d**). 45S5 showed fast hydroxyapatite-like precipitation than S53P4. However, the hydroxyapatite formation depends on the incorporation of Ca^{2+} and PO_4^{3-} on the MBG's glass surfaces during bioactivity test. Lower SiO_2 and higher CaO, P_2O_5 content in 45S5 could amplify the rate of hydroxyapatite formation on MBG's glass surfaces. The chemical composition and the microstructural morphology of 3DOM-MBGCs directly related to their bioactivity. The SBF can easier penetrate the larger macropores in the 3DOM bioactive glass compared to the mesopores in bioactive glasses [37]. Therefore, the minor difference average surface area and pore size of 3DOM-MBGCs (**Table 3**) has no effect in determining apatite growth. Due to both 3DOM-MBGCs using the same size of PMMA spheres for macroporous and same surfactant for mesoporous.

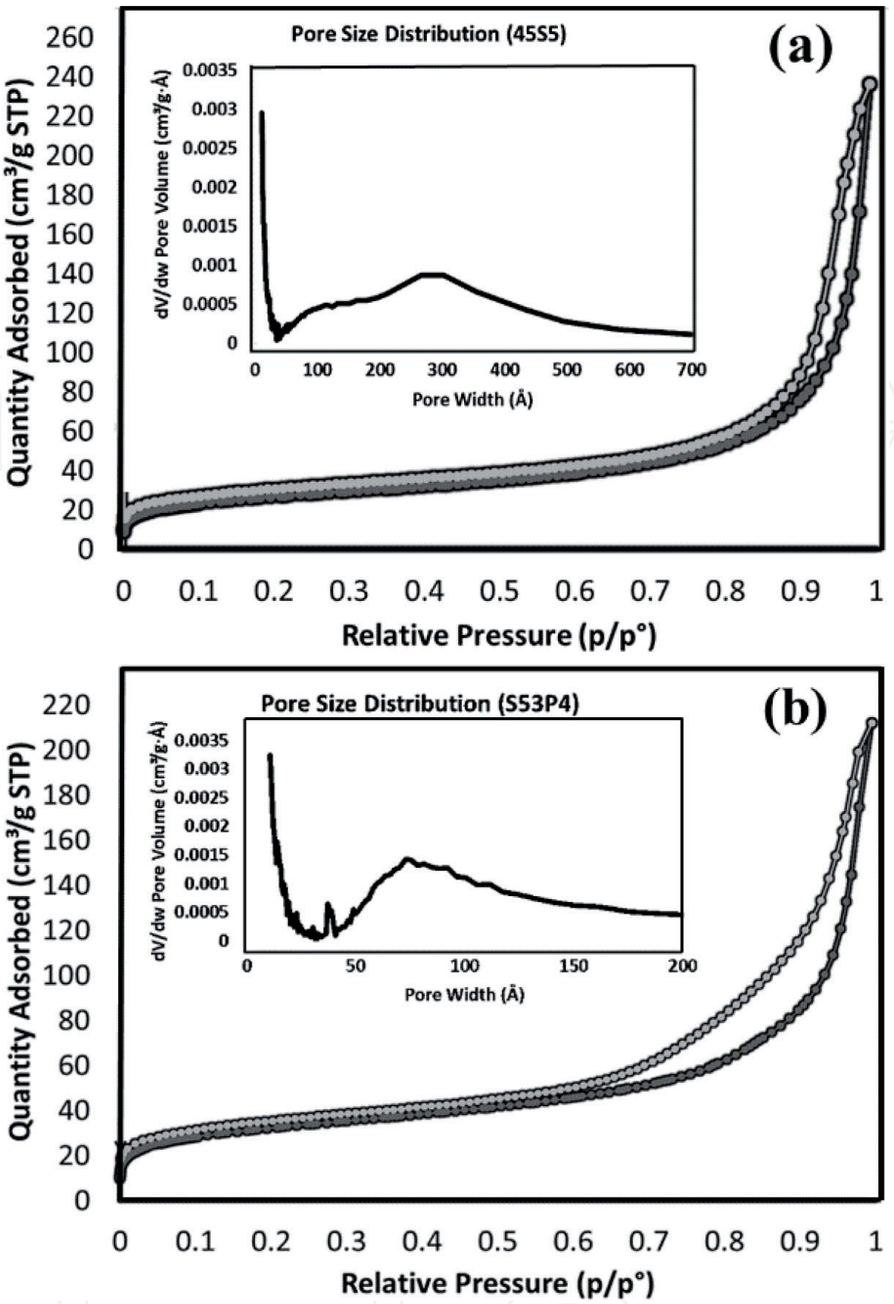

Figure 4.
N_2 adsorption–desorption isotherms and pore size distribution of (a) 45S5 and (b) S53P4 3DOM-MBGCs. Copyright [30].

Samples	Surface area (m^2/g)	Pore Volume (cm^3/g)	Pore Diameter (Å)
45S5	96.54	0.365	151.58
S53P4	116.76	0.327	112.30

Table 2.
The average data of specific surface area, pore volume and pore diameter of 45S5 and S53P4 3DOM-MBGCs. Copyright [30].

The FTIR spectra of 45S5 in **Figure** 7, at below spectrum, the sample before soaking in SBF solution exhibits the peaks at 467, 802 and 1086 cm^{-1} corresponding to the vibration of Si-O-Si bond, bending, symmetric and asymmetric stretching vibration, respectively. In vibrational peak at 564 and 950 cm^{-1} correlates to the P-O vibrational peak. In addition, the O-H bonds of the water trapped inside

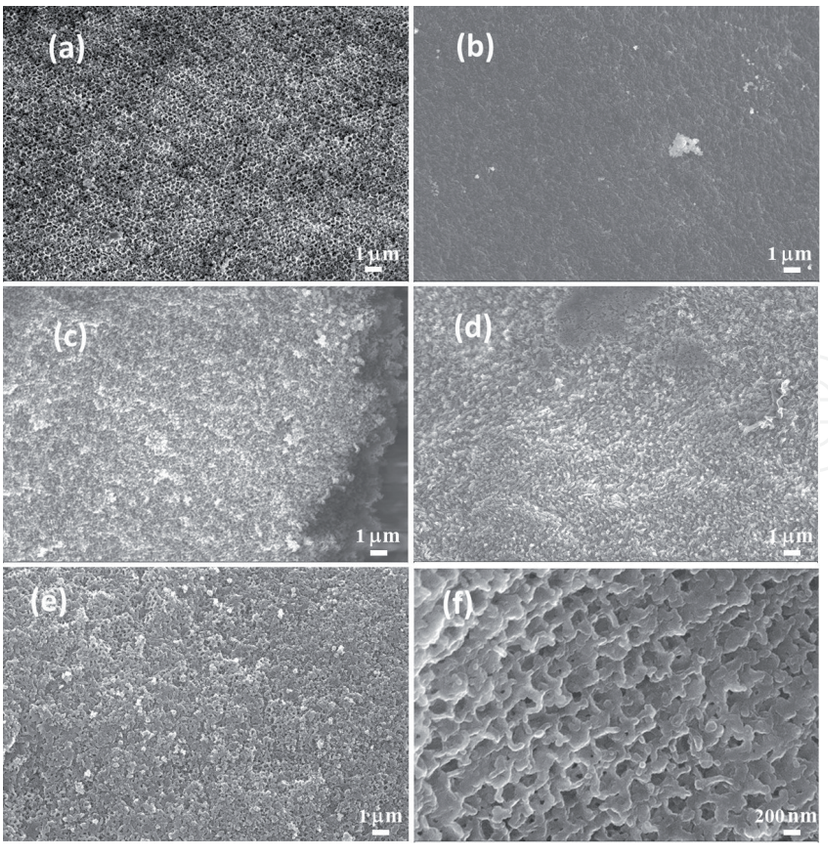

Figure 5.
SEM images of 45S5 bioactive glass ceramics (a) before soaking in SBF solution and after soaking in SBF solution for (b) 1 day (c) 2 days (d) 3 days (e) 7 days and (f) 7 days with higher magnification. Copyright [30].

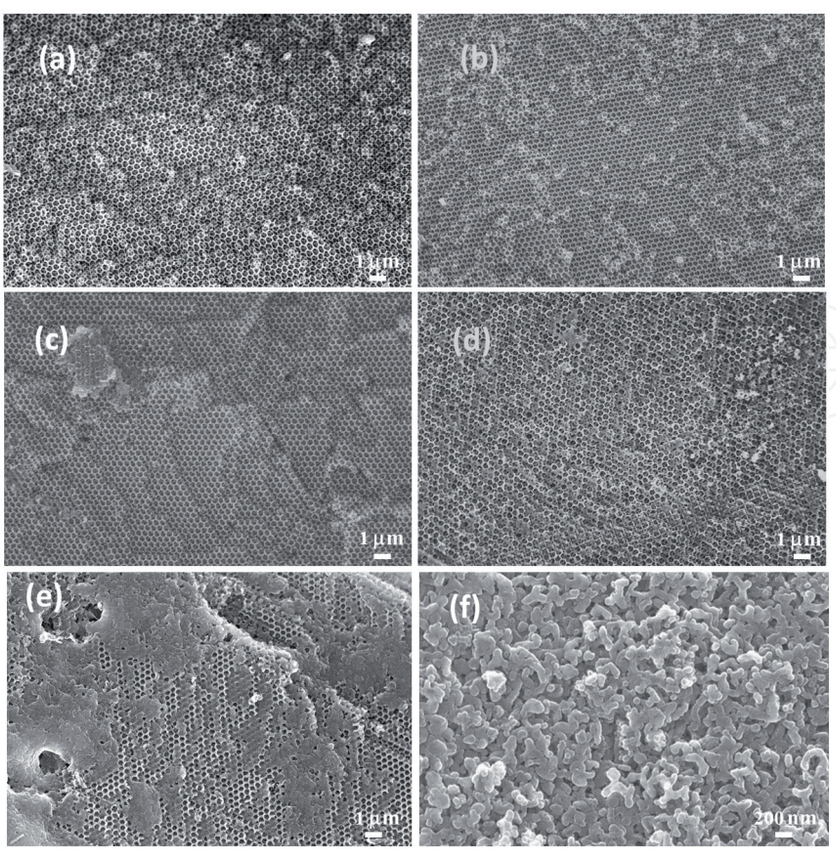

Figure 6.
SEM images of S53P4 bioactive glass ceramics (a) before soaking in SBF solution and after soaking in SBF for (b) 1 day (c) 2 days (d) 3 days (e) 7 days and (f) 7 days with higher magnification. Copyright [30].

MBGC Samples	Drug Loading efficiency (%)	Drug Loading Content (wt. %)
45S5	18.00 ± 3.16	8.74 ± 1.09
S53P4	22.14 ± 2.53	11.91 ± 2.09

Table 3.
The drug loading efficiency and content of 45S5 and S53P4.

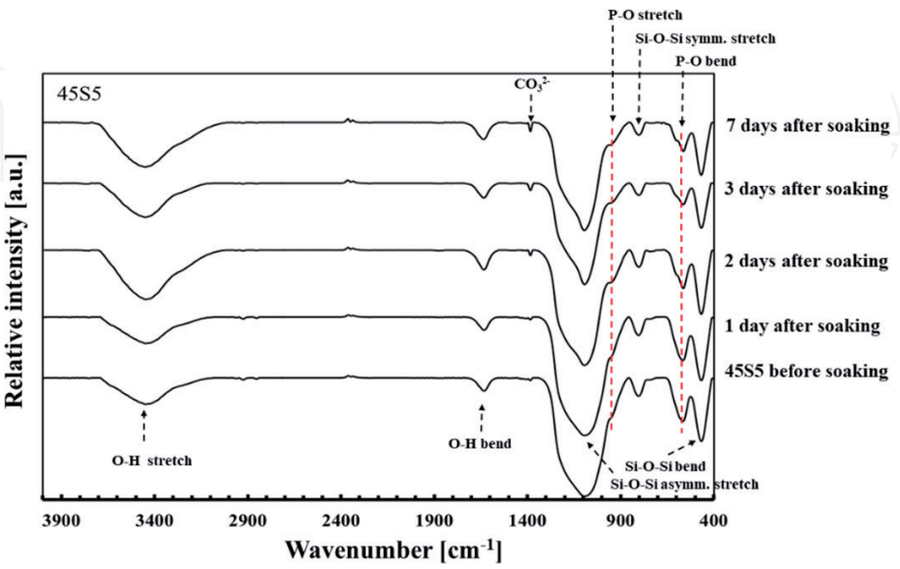

Figure 7.
FTIR spectra of 45S5 bioactive glass ceramics with different soaking time in SBF solution. Copyright [30].

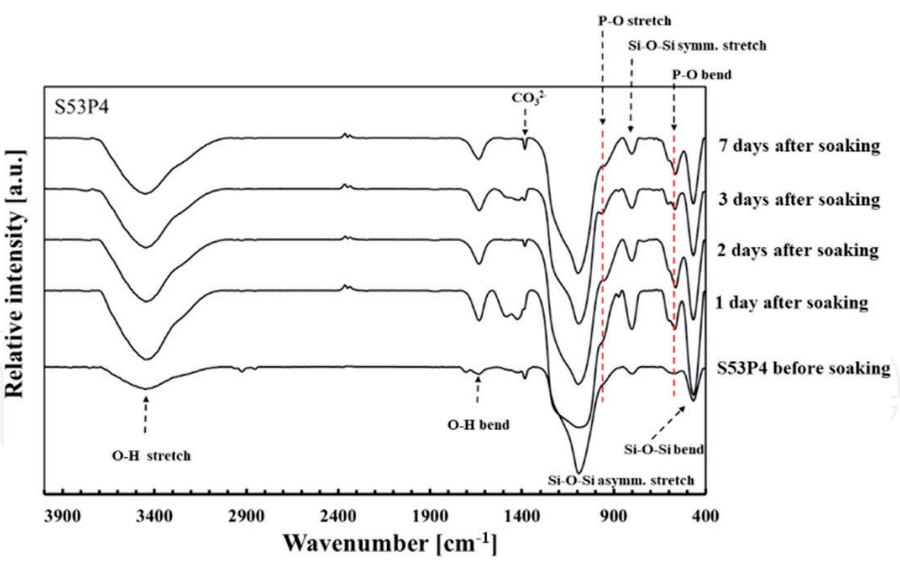

Figure 8.
FTIR spectra of S53P4 bioactive glass ceramics with different soaking time in SBF solution. Copyright [30].

the sample was shown at 1635 and 3450 cm^{-1}. The narrow band near 1384 cm^{-1} indicates the characteristic of the carbonate group (CO_3^{2-}) [35]. After the soaking in SBF, all the characteristic peaks are still observed. The P-O peak at 564 splits into doublet peak at 586 and 564 cm^{-1} which normally appears after immersion of the bioactive glass in SBF solution15. All the bands corresponding to the P-O represent the formation of hydroxyapatite on the surface of MBGCs. **Figure 8** represents the FTIR spectra of S53P4 bioactive glasses. The sample before soaking in SBF solution shows peaks at 467, 1087 and the shoulder at 1087–1250 cm^{-1}

correlates to the vibration of Si-O-Si bond. The peaks at 1385 and 1401 cm^{-1} indicates the characteristics of carbonate group (CO_3^{2-}) [35]. In the peak around 576 and 966 cm^{-1} corresponding to the P-O bending and stretching vibration, respectively. In addition, the peak at 1631 and 3445 cm^{-1} correlated to O-H bonds. After S53P4 MBGCs were soaked in SBF for 1 day, the aforementioned vibrational peaks are still observed. The P-O peak at at 607 and 567 cm^{-1}, which confirmed that the formation of amorphous phosphate phase on the glass surface [29]. Although, the splitting P-O peak of S53P4 appears in 1 day after soaking in SBF, while in the case of 45S5 after soaking for 2 days. However, the formation of hydroxyapatite-like on the surface of S53P4 glasses started after 3 days of soaking in SBF solution, slowly growth comparing with 45S5, indicated the better bioactivity of 45S5 than S53P4 bioactive glasses.

3.3 *In vitro* study of drug release

3.3.1 Drug loading

The drug loading efficiency and drug loading content of both MBGCs are summarized in **Table 3**. The drug loading efficiency in 45S5 was 18.00 ± 3.16%, while S53P4 showed quite higher drug loading efficiency of about 22.14 ± 2.53%. However, the loading efficiency of S53P4 was not statistically different from that of 45S5 (independent t-test, $p > 0.05$). The drug loading content of the MBGCs was found to be 8.74 ± 1.09 wt% for 45S5 and 11.91 ± 2.09 wt% for S53P4 glasses. The significant difference was not observed for the drug loading content of 45S5 from S53P4 (independent t-test, $p > 0.05$). S53P4 provides high average drug-loading content compared with other inert carrier materials that generally have low drug-loading content (less than 10 wt%) [33]. The porous materials can be developed to fabricate high drug-loading carriers due to their promising intrinsic properties, such as large hollow interior, porous surface, high surface area and large pore volume [33]. The good drug-loading capacity obtained in this study could be related to high surface area of the carrier with porous structure as supported by the results obtained from N_2 adsorption desorption analysis.

3.3.2 In vitro drug release

The release profiles for gentamicin from the MBGCs to the PBS are represented in **Figure 9**. For both MBGCs, the release of gentamicin showed an initial fast release followed by a relatively slow subsequent release. An initial fast release of the antibiotic was observed during the first 24 hours of soaking, reaching the mean gentamicin release values of 34.53% (45S5) and 41.21% (S53P4). The subsequent release rate was quite low in comparison with the first period. However, the S53P4 bioactive glasses showed a higher initial drug release behavior than 45S5 glasses. But later, both bioactive glasses reached the same point after 96 hours of release values of 64.27% (45S5) and 64.53% (S53P4). Both S53P4 and 45S5 bioactive glasses showed a slowly continuous gentamicin release.

To study the mechanism of drug release from the MBGCs, the first 60% of gentamicin release profile was fitted in Peppas-Korsmeyer model. In this model, the value of n characterizes the release mechanism of drug as described in **Table 4**. As observed in **Table 4**, the n values of the release data of 45S5 and S53P4 glasses are 0.3992 and 0.3004, respectively. This indicated that the drug release from both systems can be described by Fickian diffusion [34]. Both MBGCs possessed porous structures with hollow interiors. The diffusion through channel might dominate the drug release from these mesoporous materials [13, 38].

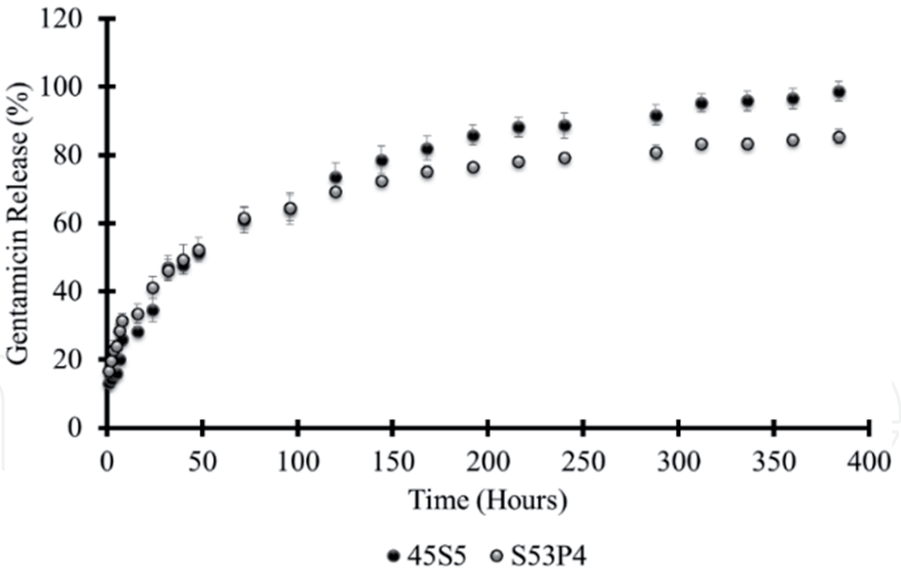

Figure 9.
In vitro gentamicin release from 45S5 and S53P4 bioactive glass ceramics.

MBG Samples	Peppas-Korsmeyer factors		
	K	*n*	R^2
45S5	0.0204	0.3992	0.95
S53P4	0.0466	0.3004	0.99

Table 4.
Kinetic assessment of gentamicin release data of 45S5 and S53P4 in PBS (Peppas-Korsmeyer model).

4. Conclusions

3DOM-MBGCs were synthesized successfully by the sol–gel method using spherical PMMA colloidal crystals of 300 nm and non-ionic block copolymer P123 as cotamplates. The morphology of S53P4 bioactive glass revealed well-ordered macroporous structure with larger surface area. While, 45S5 bioactive glass had shown distorted 3DOM structure with a bit higher pore diameter. Base on the SEM and FTIR results indicated the better bioactivity of 45S5 than S53P4 bioactive glass ceramics which was able to initiate the formation of hydroxyapatite-like layer on glass surface after soaking in SBF solution within 2 days (45S5) and 3 days (S53P4). The drug delivery system based on 45S5 and S53P4 3DOM-MBGCs have been synthesized, and the release behavior of both porous bioactive glasses were studied. The results indicated that the S53P4 glasses showed higher drug loading efficiency and gave relatively initial fast release compared to the 45S5 due to its high surface area. Even though, the drug loading content was not significant different from that of both bioactive glass ceramics. The resultant drug release mechanism was occupied from the first 60% of gentamicin release profile fitted to the Peppas-Korsmeyer model, which clarified that the kinetics of drug release from the bioactive glass ceramics mostly occurred by Fickian diffusion mechanism.

Therefore, the results indicated the bioactivity and drug release profile of mesoporous bioactive glass ceramics which can accelerate the bone growth or new bone formation and could be a use as a promising drug release system for bone implant materials preparation.

Acknowledgements

This work has been supported by Walailak University Postgraduate Scholarship for Outstanding Students (Contract no. 02/2560), financially supported by Walailak University Graduate Studies Research Fund (Contract no. 14/2561).

Conflict of interest

The authors declare no conflict of interest.

Author details

Reedwan Bin Zafar Auniq[1], Namon Hirun[2] and Upsorn Boonyang[1*]

1 Functional Materials and Nanotechnology Center of Excellence, School of Science, Walailak University, Nakhon Si Thammarat, Thailand

2 Division of Pharmaceutical Sciences, Faculty of Pharmacy, Thammasat University, Pathumthani, Thailand

*Address all correspondence to: upsorn.bo@mail.wu.ac.th

References

[1] Martin, R. A.; Yue, S.; Hanna, J. V.; Lee, P. D.; Newport, R. J.; Smith, M. E.; Jones, J. R., Characterizing the hierarchical structures of bioactive sol-gel silicate glass and hybrid scaffolds for bone regeneration. Philosophical Transactions of the Royal Society A: Mathematical, Physical and Engineering Sciences 2012, 370, 1422-1443. DOI: 10.1098/rsta.2011.0308

[2] Arcos, D.; Vallet-Regí, M., Bioceramics for drug delivery. Acta Materialia 2013, 61 (3), 890-911. DOI: 10.1016/j.actamat.2012.10.039

[3] Yan, X.; Huang, X.; Yu, C.; Deng, H.; Wang, Y.; Zhang, Z.; Qiao, S.; Lu, G.; Zhao, D., The *in-vitro* bioactivity of mesoporous bioactive glasses. Biomaterials 2006, 27 (18), 3396-3403. DOI: 10.1016/j.biomaterials.2006.01.043

[4] Jones, J. R., Reprint of: review of bioactive glass: From Hench to hybrids. Acta Biomaterialia 2015, 23, S53-S82. DOI: 10.1016/j.actbio.2015.07.019

[5] Hench, L. L., Chronology of bioactive glass development and clinical applications. New Journal of Glass and Ceramics 2013, 3 (2), 67-73. DOI: 10.4236/njgc.2013.32011

[6] Li, X.; Wang, X.; Chen, H.; Jiang, P.; Dong, X.; Shi, J., Hierarchically porous bioactive glass scaffolds synthesized with a PUF and P123 cotemplated approach. Chemistry of Materials 2007, 19 (17), 4322-4326. DOI:10.1021/cm0708564

[7] Li, R.; Clark, A. E.; Hench, L. L., An investigation of bioactive glass powders by sol-gel processing. Journal of Applied Biomaterials 1991, 2 (4), 231-239. DOI: 10.1002/jab.770020403

[8] Jones, J. R.; Lin, S.; Yue, S.; Lee, P. D.; Hanna, J. V.; Smith, M. E.; Newport, R. J., Bioactive glass scaffolds for bone regeneration and their hierarchical characterisation. Proceedings of the Institution of Mechanical Engineers, Part H 2010, 224 (12), 1373-87. DOI: 10.1243/09544119JEIM836

[9] Vallet-Regí, M.; Ragel, C. V.; Salinas, Antonio J., Glasses with medical applications. European Journal of Inorganic Chemistry 2003, 2003 (6), 1029-1042. DOI: 10.1002/ejic.200390134

[10] Sepulveda, P.; Jones, J. R.; Hench, L. L., Characterization of melt-derived 45S5 and sol-gel–derived 58S bioactive glasses. Journal of Biomedical Materials Research 2001, 58 (6), 734-740. DOI: 10.1002/jbm.10026

[11] Sharifianjazi, F.; Parvin, N.; Tahriri, M., Formation of apatite nano-needles on novel gel derived SiO_2-P_2O_5-CaO-SrO-Ag_2O bioactive glasses. Ceramics International 2017, 43 (17), 15214-15220. DOI: 10.1016/j.ceramint.2017.08.056

[12] Gupta, R.; Kumar, A., Bioactive materials for biomedical applications using sol–gel technology. Biomedical Materials 2008, 3 (3), 034005. DOI: 10.1088/1748-6041/3/3/034005

[13] Wu, C.; Chang, J., Mesoporous bioactive glasses: structure characteristics, drug/growth factor delivery and bone regeneration application. Interface Focus 2012, 2 (3), 292-306. DOI: 10.1098/rsfs.2011.0121

[14] Xia, W.; Chang, J., Well-ordered mesoporous bioactive glasses (MBG): a promising bioactive drug delivery system. Journal of Controlled Release 2006, 110 (3), 522-530. DOI: 10.1016/j.jconrel.2005.11.002

[15] Liu, Y.-Z.; Li, Y.; Yu, X.-B.; Liu, L.-N.; Zhu, Z.-A.; Guo, Y.-P., Drug delivery property, bactericidal property and cytocompatibility of magnetic mesoporous bioactive glass.

Materials Science and Engineering: C 2014, 41, 196-205. DOI: 10.1016/j.msec.2014.04.037

[16] Zhang, X.; Zhang, J.; Shi, B., Mesoporous bioglass/silk fibroin scaffolds as a drug delivery system: Fabrication, drug loading and release *in vitro* and repair calvarial defects *in vivo*. Journal of Wuhan University of Technology-Mater. Sci. Ed. 2014, 29 (2), 401-406. DOI: 10.1007/s11595-014-0929-0

[17] Huang, C.-Y.; Huang, T.-H.; Kao, C.-T.; Wu, Y.-H.; Chen, W.-C.; Shie, M.-Y., Mesoporous calcium silicate nanoparticles with drug delivery and odontogenesis properties. Journal of Endodontics 2017, 43 (1), 69-76. DOI: 10.1016/j.joen.2016.09.012

[18] Wu, C.; Chang, J., Multifunctional mesoporous bioactive glasses for effective delivery of therapeutic ions and drug/growth factors. Journal of Controlled Release 2014, 193, 282-295. DOI: 10.1016/j.jconrel.2014.04.026

[19] Yan, X.; Yu, C.; Zhou, X.; Tang, J.; Zhao, D., Highly ordered mesoporous bioactive glasses with superior *in vitro* bone-forming bioactivities. Angewandte Chemie International Edition 2004, 43 (44), 5980-5984. DOI: 10.1002/anie.200460598

[20] Zhu, Y.; Kaskel, S., Comparison of the *in vitro* bioactivity and drug release property of mesoporous bioactive glasses (MBGCs) and bioactive glasses (BGs) scaffolds. Microporous and Mesoporous Materials 2009, 118 (1), 176-182. DOI: 10.1016/j.micromeso.2008.08.046

[21] Li, Y.; Liu, Y.-Z.; Long, T.; Yu, X.-B.; Tang, T. T.; Dai, K.-R.; Tian, B.; Guo, Y.-P.; Zhu, Z.-A., Mesoporous bioactive glass as a drug delivery system: fabrication, bactericidal properties and biocompatibility. Journal of Materials Science: Materials in Medicine 2013, 24 (8), 1951-1961. DOI: 10.1007/s10856-013-4960-z

[22] Kaur, G.; Pandey, O. P.; Singh, K.; Homa, D.; Scott, B.; Pickrell, G., A review of bioactive glasses: Their structure, properties, fabrication and apatite formation. Journal of Biomedical Materials Research Part A 2014, 102 (1), 254-274. DOI: 10.1002/jbm.a.34690

[23] Li, W.; Nooeaid, P.; Roether, J. A.; Schubert, D. W.; Boccaccini, A. R., Preparation and characterization of vancomycin releasing PHBV coated 45S5 Bioglass®-based glass–ceramic scaffolds for bone tissue engineering. Journal of the European Ceramic Society 2014, 34 (2), 505-514. DOI: 10.1016/j.biomaterials.2011.01.004

[24] Hoppe, A.; Güldal, N. S.; Boccaccini, A. R., A review of the biological response to ionic dissolution products from bioactive glasses and glass-ceramics. Biomaterials 2011, 32 (11), 2757-2774. DOI:

[25] Wen, H.; Jung, H.; Li, X., Drug Delivery Approaches in Addressing Clinical Pharmacology-Related Issues: Opportunities and Challenges. AAPS J 2015, 17 (6), 1327-1340. DOI: 10.1208/s12248-015-9814-9

[26] Liu, W.; Chang, J., *In vitro* evaluation of gentamicin release from a bioactive tricalcium silicate bone cement. Materials Science and Engineering: C 2009, 29 (8), 2486-2492. DOI: 10.1016/j.msec.2009.07.015

[27] Dorati, R.; DeTrizio, A.; Genta, I.; Grisoli, P.; Merelli, A.; Tomasi, C.; Conti, B., An experimental design approach to the preparation of pegylated polylactide-co-glicolide gentamicin loaded microparticles for local antibiotic delivery. Materials Science and Engineering: C 2016, 58, 909-917. DOI: 10.1016/j.msec.2015.09.053

[28] Perni, S.; Martini-Gilching, K.; Prokopovich, P., Controlling release kinetics of gentamicin from silica nano-carriers. Colloids and Surfaces A: Physicochemical and Engineering Aspects 2018, 541, 212-221. DOI: 10.1016/j.colsurfa.2017.04.063

[29] Boonyang, U.; Li, F.; Stein, A., Hierarchical structures and shaped particles of bioactive glass and its *in vitro* bioactivity. Journal of Nanomaterials 2013, 2013 (Article ID 681391), 1-6. DOI: 10.1155/2013/681391

[30] Auniq, R. B.-Z.; Pakasri, N.; Boonyang, U., Synthesis and *in vitro* bioactivity of three-dimensionally ordered macroporous-mesoporous bioactive glasses; 45S5 and S53P4. Journal of the Korean Ceramic Society 2020. DOI: 10.1007/s43207-020-00050-z

[31] Kokubo, T.; Takadama, H., How useful is SBF in predicting *in vivo* bone bioactivity? Biomaterials 2006, 27 (15), 2907-2915. DOI: 10.1016/j.biomaterials.2006.01.017

[32] Zhang, X.; Wyss, U. P.; Pichora, D.; Goosen, M. F. A., An Investigation of poly (lactic acid) degradation. Journal of Bioactive and Compatible Polymers 1994, 9 (1), 80-100. DOI: 10.1177/088391159400900105

[33] Shen, S.; Wu, Y.; Liu, Y.; Wu, D., High drug-loading nanomedicines: progress, current status, and prospects. International Journal of Nanomedicine 2017, 12, 4085-4109. DOI: 10.2147/IJN.S132780

[34] Soundrapandian, C.; Datta, S.; Kundu, B.; Basu, D.; Sa, B., Porous bioactive glass scaffolds for local drug delivery in osteomyelitis: Development and *in vitro* characterization. AAPS PharmSciTech 2010, 11 (4), 1675-1683. DOI: 10.1208/s12249-010-9550-5

[35] Lucas-Girot, A.; Mezahi, F. Z.; Mami, M.; Oudadesse, H.; Harabi, A.; Le Floch, M., Sol–gel synthesis of a new composition of bioactive glass in the quaternary system SiO_2–CaO–Na_2O–P_2O_5: Comparison with melting method. Journal of Non-Crystalline Solids 2011, 357 (18), 3322-3327. DOI: 10.1016/j.jnoncrysol.2011.06.002

[36] Alothman, Z. A., A Review: Fundamental sspects of silicate mesoporous Materials. Materials 2012, 5 (12), 2874-2902. DOI: 10.3390/ma5122874

[37] Bell, D. C.; Zhang, K.; Yan, H.; Francis, L. F.; Stein, A., Three dimensionally ordered macroporous bioactive glasses. Microscopy and Microanalysis 2002, 8 (S02), 330-331. DOI: 10.1017/S1431927602100900

[38] Xichen, Z.; Wyss, U. P.; Pichora, D.; Goosen, M. F. A., A mechanistic study of antibiotic release from biodegradable poly(d,1-lactide) cylinders. Journal of Controlled Release 1994, 31 (2), 129-144. DOI: 10.1016/0168-3659(94)00011-5